

Elastic Interactions of Cells

U. S. Schwarz¹ and S. A. Safran²

¹*Max-Planck-Institute of Colloids and Interfaces, 14424 Potsdam, Germany*

²*Department of Materials and Interfaces, The Weizmann Institute of Science, Rehovot 76100, Israel*

Biological cells in soft materials can be modeled as anisotropic force contraction dipoles. The corresponding elastic interaction potentials are long-ranged ($\sim 1/r^3$ with distance r) and depend sensitively on elastic constants, geometry and cellular orientations. On elastic substrates, the elastic interaction is similar to that of electric quadrupoles in two dimensions and for dense systems leads to aggregation with herringbone order on a cellular scale. Free and clamped surfaces of samples of finite size introduce attractive and repulsive corrections, respectively, which vary on the macroscopic scale. Our theory predicts cell reorientation on stretched elastic substrates.

Biological cells can exert strong physical forces on their surroundings. One example are fibroblasts, which are mechanically active cells found in connective tissue. In the early 1980s, Harris and coworkers found that fibroblasts exert much more force than needed for locomotion [1]. They suggested that strong fibroblast traction is needed in order to align the collagen fibers in the connective tissue. Since cell locomotion is guided by collagen fibers, this results in a *mechanical interaction* of cells. The interplay of fiber alignment and cell locomotion has been analyzed theoretically in the framework of coupled transport equations for fiber and cell degrees of freedom [2]. However, it is well known that cellular behavior is also affected by purely elastic effects, which were not considered in these studies. For example, stationary cells plated on an elastic substrate which is cyclically stretched reorientate away from the stretching direction [3], and locomoting cells on a strained elastic substrate reorientate in the strain direction [4]. Recent experiments show that adhering cells sense mechanical signals through focal adhesions [5]. In contrast to chemical diffusion fields, elastic effects are long-ranged and propagate quickly, and they are known to be important during development, wound healing, inflammation and metastasis [6].

In this Letter, we consider theoretically the possibility of *elastic interaction* of cells. We focus on static forces, a situation which should apply to cells with restricted cytoskeletal regulation or to artificial cells which have a biomimetic contractile system without any regulation; the theoretical framework presented here for this case is a prerequisite for understanding the more complicated cases, e.g. the case of locomoting cells with a regulated response and dynamic force patterns [4]. In the static case, the elastic interaction of cells through their strain fields leads to forces and torques which can change their positions and orientations. If the cellular configuration can relax to equilibrium, the final configuration will be a minimum of the elastic energy. In the following, we derive the laws for elastic interactions of cells (which are modeled as anisotropic force contraction dipoles) and show how they depend on elastic constants, distance, cellular orientations, geometry and boundary conditions.

If the distance between cells is much larger than their

spatial extent, they can be modeled as point defects in an elastic medium. Elastic interactions of point defects have been discussed before for e.g. hydrogen in metal [7], atoms adsorbed onto crystal surfaces [8], and graphite intercalation compounds [9]. For each defect, the force is restricted to a small region of space, and the force distribution can be characterized by its *force multipoles* [10]

$$P_{i_1 \dots i_n i} = \int s_{i_1} \dots s_{i_n} f_i(\mathbf{s}) d\mathbf{s} \quad (1)$$

where \mathbf{f} is the force density. The force monopole \mathbf{P} is the overall force, which vanishes for inert particles. Therefore in the classical case, the first relevant term is the force dipole P_{ij} , which describes the dilating/contracting action of the force distribution and has the dimension of an energy. Previous studies of elastic interactions of force multipoles were mostly concerned with *isotropic* force *dilation* dipoles (that is $P_{ij} = P\delta_{ij}$ with $P > 0$) and the finite sample size effect of *free* surfaces. The biological case which we discuss here is different in several respects. First, since cells can act as active walkers, there exists the possibility of force monopoles. Second, cellular force is based on actomyosin contractility and therefore leads to force *contraction* dipoles (that is $P < 0$). Third, adhering cells in most cases generate highly *anisotropic* force patterns, that is, the force dipole is not isotropic and will reorientate with respect to the surrounding strain field (e.g. on strained substrates). And fourth, in biological cases the elastic medium (e.g. the tissue) has *clamped* rather than free surfaces. In fact it is well known that cells become mechanically active only if their environment can support enough stress, thus clamped boundary conditions are often needed to induce cellular activation [11].

We assume that the elastic medium of interest (real or artificial tissues, elastic substrates) propagates strain like an isotropic elastic medium with a Young modulus in the order of kPa. For elastic substrates, the Poisson ratio ν is close to 1/2 (incompressible case). For the following it is convenient to define $\Lambda = \lambda/\mu$ and $c = 2\mu + \lambda = \mu(2 + \Lambda)$, where μ and λ are the Lamé coefficients of the isotropic elastic medium. The incompressible case $\nu = \Lambda/2(\Lambda + 1) = 1/2$ then corresponds to

the limit $\Lambda \rightarrow \infty$ with $\Lambda/c \rightarrow 1/\mu$. Propagation of strain in an infinite isotropic elastic medium is described by the Green function [12]

$$G_{ij}^{3d} = \frac{1}{8\pi c} \left\{ (3 + \Lambda)\delta_{ij} + (1 + \Lambda)\frac{x_i x_j}{r^2} \right\} \frac{1}{r} \quad (2)$$

where r denotes the distance from the force center. For cells plated on an elastic substrate with a substrate thickness that is much larger than the displacements caused by cell traction, the relevant Green function is the one of an isotropic elastic halfspace with a free surface. Since such cells apply only tangential traction, we need to specify G_{ij} only for the x-y-plane [12]:

$$G_{ij}^{2d} = \frac{(2 + \Lambda)}{4\pi(1 + \Lambda)c} \left\{ (2 + \Lambda)\delta_{ij} + \Lambda\frac{x_i x_j}{r^2} \right\} \frac{1}{r}. \quad (3)$$

The elastic interaction energy W between two force distributions can be written as a function of their force multipoles and the Green function [10]

$$\begin{aligned} W &= - \int \int f_i(\mathbf{s}) G_{ij}(|\mathbf{s} - \mathbf{s}'|) f_j(\mathbf{s}') ds ds' \\ &= - \sum_{n=0}^{\infty} \sum_{m=0}^{\infty} \frac{1}{n!} \frac{(-1)^m}{m!} G_{ij,i_1 \dots i_n j_1 \dots j_m} P_{i_1 \dots i_n} P'_{j_1 \dots j_m} \end{aligned} \quad (4)$$

where we sum over repeated indices and where indices after the comma represent partial derivatives. In the second line, the first line has been expanded twice and the definitions of Eq. (1) have been used.

The interaction between two force monopoles \mathbf{P} and \mathbf{P}' at \mathbf{r} and \mathbf{r}' , respectively, follows from Eq. (4) as $W = -P_i G_{ij}(\mathbf{r} - \mathbf{r}') P'_j$. In the incompressible limit, this can be written as $W = -(\mathbf{P} \cdot \mathbf{P}' + (\mathbf{P} \cdot \mathbf{n})(\mathbf{P}' \cdot \mathbf{n}))/8\pi\mu r$, where \mathbf{n} is the normalized separation vector between the two monopole locations (in three dimensions; in two dimensions, an additional factor of 2 appears). This interaction is similar to the one between electric dipoles [13], thus we expect chaining to dominate large scale assembly, as confirmed by Monte Carlo simulations (not shown). However, since the force monopoles correspond to active movements, a model for cell locomotion is required to fully treat this case.

It is generally accepted that mechanically active cells exert only a very small overall force. Moreover, in most cases they are usually found to have highly polarized, that is, pinching force patterns [14]. In the following we therefore model cellular force patterns as anisotropic force contraction dipoles. The direction $\hat{\mathbf{r}}$ of the pinch can be extracted from experimentally measured force patterns by determining the direction of the eigenvector of the force dipole tensor corresponding to its largest eigenvalue. Then the force dipole tensor can be approximated as $P_{ij} = P\hat{r}_i\hat{r}_j$. In many cases, the cell orientation following from the force pattern corresponds to

the cell orientation following from overall cell shape or staining for actin fibers. For both locomoting and stationary fibroblasts on elastic substrates, the magnitude of the force dipole can be estimated to be of the order of $P \approx -10^{-11} J$ (this corresponds to a pinching pair of forces, separated by a distance of 60 μm and each 200 nN strong). The corresponding length scale (e.g. for displacements close to the cell) is $(P/c)^{1/3} \approx 10 \mu\text{m}$, which is somewhat smaller than a typical cell size ($\approx 50 \mu\text{m}$). The interaction between two force dipoles P_{li} and P'_{kj} at \mathbf{r} and \mathbf{r}' , respectively, follows from Eq. (4) as

$$W(\mathbf{r}, \mathbf{r}') = -P_{li} u_{i,l}(\mathbf{r}, \mathbf{r}') = P_{li} G_{ij,lk}(\mathbf{r} - \mathbf{r}') P'_{kj} \quad (5)$$

where $\mathbf{u}(\mathbf{r}, \mathbf{r}')$ is the displacement at \mathbf{r} produced by the force dipole at \mathbf{r}' . Since $G \sim 1/r$, the elastic interaction between force dipoles scales as $\sim 1/r^3$.

If the cells have isotropic force dipoles, their elastic interactions are well known: in infinite space, $W = P^2 G_{ij,ij}^{3d} = 0$ [10] and an elastic interaction can only be induced by the boundary conditions [7]. On a semi-infinite space with free surface, $W = P^2 G_{ij,ij}^{2d} = (2 + \Lambda)^2 P^2 / 4\pi(1 + \Lambda)cr^3$, thus the interaction is isotropic and repulsive [8]. However, in most cases the cells will have highly anisotropic force dipoles. We start with the half-space and consider the following situation: one of the two interacting dipoles is fixed at the origin with vanishing polar angle. The other dipole is a distance r away with polar angle α . The polar angle of the separation vector is denoted by β . Using Eq. (3) in Eq. (5), we find

$$W(r, \alpha, \beta) = \frac{(2 + \Lambda)P^2}{4\pi c(1 + \Lambda)r^3} f(\alpha, \beta) \quad (6)$$

with

$$\begin{aligned} f(\alpha, \beta) &= \frac{1}{8} [(4 + 3\Lambda) \cos(2\alpha) + 15\Lambda \cos(2(\alpha - 2\beta)) \\ &\quad + (2 + \Lambda)(2 + 6 \cos(2(\alpha - \beta)) + 6 \cos(2\beta))] . \end{aligned} \quad (7)$$

Depending on orientation, the interaction can be repulsive or attractive. The attractive component leads to orientation dependent aggregation.

In order to investigate this point in more detail, we consider force dipoles with a spherical hard core (corresponding to a typical cell size). For $\Lambda \approx 0$ (vanishing Poisson ratio), the only favorable alignments will be side-by-side and the cells will assemble into linear strings, with their orientations perpendicular to the string direction. For larger Λ , aggregation will be much more compact. In the incompressible case, for a given angle β the optimal angle α follows as $\alpha_{min} \approx \pi/2 + 2\beta$; the corresponding f varies between -2 and -1.4. The optimal energy -2 is obtained for the four perpendicular configurations. Considering only nearest neighbor interactions would lead to a square lattice at higher densities. However, at area densities beyond $\pi/4$, this structure is overpacked and a

herringbone structure results. Although the herringbone structure does not achieve the lower energy values of the square lattice, it can exist up to area density $\pi/2\sqrt{3}$ and will be favored for entropic reasons. For finite-sized clusters, surface reconstruction will take place. Moreover, for an increasing number of particles the interaction of Eq. (6) leads to an increasingly rugged energy landscape with many local minima due to the long range and orientation dependence of the potential. As a result of this metastability, unusual patterns like rings will form for certain initial conditions. In Fig. 1 we show some typical configurations.

It is instructive to note that the orientational part of the interaction in the incompressible limit is very similar to that of linear electric quadrupoles in two dimensions (see Fig. 1). This analogy is due to the fact that the corresponding interaction energy for linear electric quadrupoles, $W = G_{ijkl}^{el} P_{ij} P'_{kl}$ (where $G^{el}(r) \sim 1/r$ is the electric Green function), arises from contracting tensors of analogous symmetry. However, the near perfect agreement in the angle-dependent part is an accidental result for the incompressible case; moreover, electric quadrupoles interact with $1/r^5$ rather than with $1/r^3$.

We now discuss the elastic interaction of anisotropic force contraction dipoles acting in a three-dimensional elastic medium, which follows by using Eq. (2) in Eq. (5). This interaction is more complicated than the two-dimensional one, since its orientation dependence involves three rather than two different angles. A detailed discussion will be given elsewhere. Here we only discuss some high symmetry cases: for two parallel dipoles pointing in z-direction and placed along the x-axis, we find

$$W^{direct}(x) = \frac{(\Lambda - 1)P^2}{8\pi c x^3}. \quad (8)$$

Thus this interaction changes sign as Λ varies through 1 ($\nu = 1/4$). If one considers force dipoles arranged around a central dipole in the x-z-plane, similar considerations apply as in the two-dimensional case: for example, when considering only nearest neighbor interactions, a square arrangement of perpendicular dipoles with interaction energy $W(r) = -(\Lambda + 1)P^2/4\pi c r^3$ is the most favorable one. However, if one now tries to continue this arrangement in the third dimension, frustration effects result. Depending on initial conditions, this enhances the occurrence of irregular patterns.

Due to the long-ranged nature of the elastic interaction, boundary effects will be very important [7,15]. As an instructive example, we now discuss the elastic interaction of anisotropic force contraction dipoles in an isotropic elastic sphere of macroscopic radius R . For a free surface, this situation has been investigated before for both isotropic [7] and anisotropic force dipoles [16]. However, no such treatment exists for clamped surfaces, which are expected to have larger biological relevance. For both free and clamped surfaces, one has to introduce

image displacements, which can be determined using expansions in vector spherical harmonics [16]. Again the general expressions will be given elsewhere, and here we only consider the high symmetry case of two dipoles both orientated in z-direction. Their direct interaction along the x-axis is given by Eq. (8). The image interaction follows from inserting the image displacements of the first dipole (which are complicated functions expressed as vector spherical harmonics) into Eq. (5). For simplicity, here we report only the results for the incompressible limit. We find

$$W_{free}^{img}(x) = \frac{P^2}{76\pi\mu R^3}(-45 + 48\left(\frac{x}{R}\right)^2) \quad (9)$$

for a free surface and

$$W_{clamped}^{img}(x) = \frac{P^2}{20\pi\mu R^3}(2 - 15\left(\frac{x}{R}\right)^2) \quad (10)$$

for a clamped surface. Therefore free and clamped surfaces introduce attractive and repulsive corrections, respectively. In Fig. 2 we show the interaction energies W for $\Lambda = 2$ ($\nu = 1/3$) as a function of distance x . We see that the image corrections can produce new minima in the full interaction potential. The main conclusion from Eqs. (9,10) is the fact that the image effects lead to corrections which operate on the macroscopic scale R . For the case of hydrogen in metal, this is known to lead to structure formation on a macroscopic scale (*macroscopic modes*) [7,15]. In the biological case, the boundary induced pattern formation competes with structure formation on cellular and elastic scales, which results from the direct elastic interaction. Therefore we expect that in a theory for cellular densities modes in elastic media of finite size, hierarchical structures will result. Like for hydrogen in metal, image effects can be also expected to lead to incoherent deformations (fracture).

The simplest case of the interaction of a cellular force pattern with an elastic strain field is the case of a single cell plated on an elastic substrate which is homogeneously stretched along the x-direction by applying stress $p > 0$ at the sides. Then $(u_x, u_y) = (p/E)(x, -\nu y)$, with E being the Young modulus. The interaction energy follows as $W = -P_{li}u_{i,l} = -(Pp/E)(\cos^2\alpha - \nu\sin^2\alpha)$, where α is the polar angle describing cell orientation. Since $P < 0$, the cell will reorientate *perpendicular* to the direction of stretching ($\alpha = 90^\circ$). In the case of compression, $p < 0$, the cell will reorientate *parallel* to the direction of compression ($\alpha = 0^\circ$). Although the dynamic aspects of elastic interactions of cells are out of the scope of the present work, it is worth noting that on cyclically stretched elastic substrates, p periodically changes sign and in order to maintain a stationary state, the cell might try to avoid both tensile and compressive strain. One easily calculates that this corresponds to $\alpha = \arccos\sqrt{\nu/(1+\nu)}$. For $\nu \approx 0.4$, this yields $\alpha \approx 60^\circ$, in excellent agreement with experiments [3].

Acknowledgments: It is a pleasure to thank N. Q. Balaban, A. Bershadsky, P. Fratzl, B. Geiger, D. Riveline and T. Tlusty for helpful discussions. USS thanks the Minerva Foundation and the Emmy Noether Program of the German Science Foundation for support. SAS thanks the Schmidt Minerva Center and the Center on Self-Assembly sponsored by the Israel Science Foundation.

-
- [1] A. K. Harris, P. Wild, and D. Stopak, *Science*, 208:177–179, 1980; A. K. Harris, D. Stopak, and P. Wild, *Nature*, 290:249–251, 1981.
 - [2] G. F. Oster, J. D. Murray, and A. K. Harris, *J. Embryol. Exp. Morph.*, 78:83–125, 1983; V. H. Barocas and R. T. Tranquillo, *J. Biomech. Eng.*, 119:137–145, 1997.
 - [3] P. C. Dartsch, H. Hämmerle and E. Betz, *Acta anat.* 125:108–113 (1986); J. H.-C. Wang and E. S. Grood, *Connect. Tissue Res.* 41:29–36 (2000).
 - [4] C.-M. Lo et al., *Biophys. J.*, 79:144–152, 2000.
 - [5] N. Q. Balaban et al., *Nature Cell Biol.* 3:466–472, 2001; D. Riveline et al., *J. Cell Bio.*, 153:1175–1185, 2001.
 - [6] M. E. Chicurel, C. S. Chen and D. E. Ingber, *Curr. Opin. Cell Biol.*, 10:232–239, 1998; C. G. Galbraith and M. Sheetz, *Curr. Opin. Cell Biol.*, 10:566–571, 1998.
 - [7] H. Wagner and H. Horner, *Adv. Phys.*, 23:587, 1974.
 - [8] K. H. Lau and W. Kohn, *Surf. Sci.*, 65:607–618, 1977.
 - [9] S. A. Safran and D. R. Hamann, *Phys. Rev. Lett.*, 42:1410–1413, 1979.
 - [10] R. Siems, *Phys. Stat. Sol.*, 30:645–658, 1968.
 - [11] F. Grinnell, *Trends in Cell Biol.*, 10:362–365, 2000.
 - [12] L. D. Landau and E. M. Lifshitz, *Theory of elasticity*, Pergamon Press, Oxford, 2nd edition, 1970.
 - [13] P. G. de Gennes and P. A. Pincus, *Phys. Kondens. Materie*, 11:189–198, 1970; T. Tlusty and S. A. Safran, *Science*, 290:1328–1331, 2000.
 - [14] M. Dembo and Y.-L. Wang, *Biophys. J.*, 76:2307–2316, 1999; T. Oliver, M. Dembo, and K. Jacobson, *J. Cell Biol.*, 145:589–604, 1999; N. Q. Balaban and U. S. Schwarz, unpublished.
 - [15] H. Zabel and H. Peisl, *Phys. Rev. Lett.*, 42:511–514, 1979.
 - [16] R.-P. Hirsekorn and R. Siems, *Z. Phys. B - Cond. Mat.*, 40:311–319, 1981.

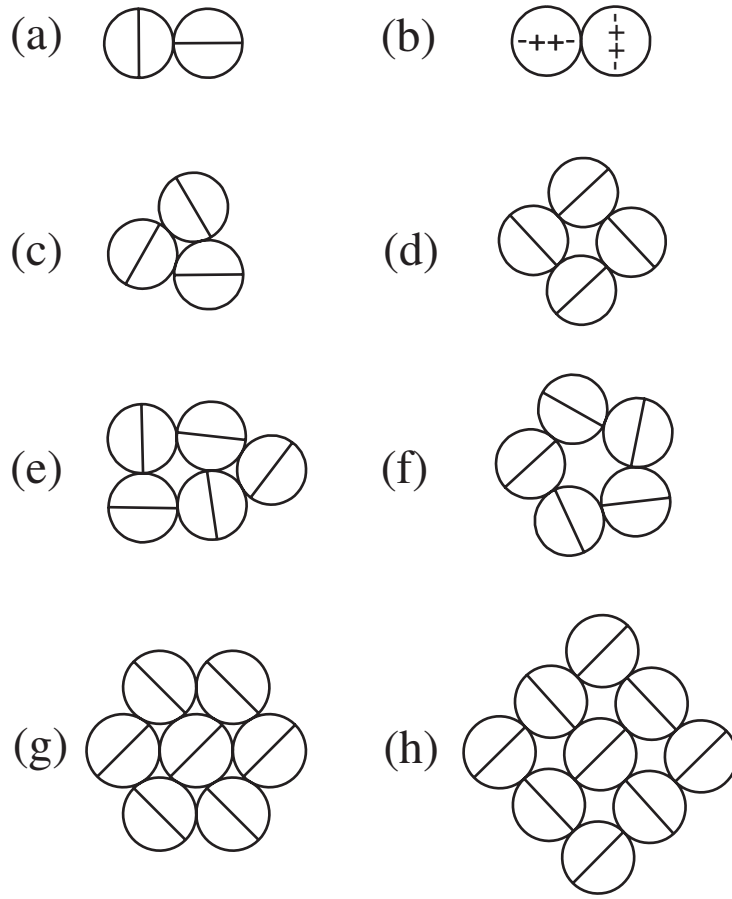


FIG. 1. Typical configurations for anisotropic force dipoles on an incompressible elastic substrate. (a) Minimal energy configuration for two dipoles ($f = -2$). (b) Linear electric quadrupoles have the same optimal configuration. (c) - (f) Small clusters are subject to surface reconstruction. For five particles, (e) and (f) are nearly degenerate ($f = -11.59$ and $f = -11.43$, respectively). (g) At high densities, herringbone order results. (h) In terms of energy, the square lattice is most favorable.

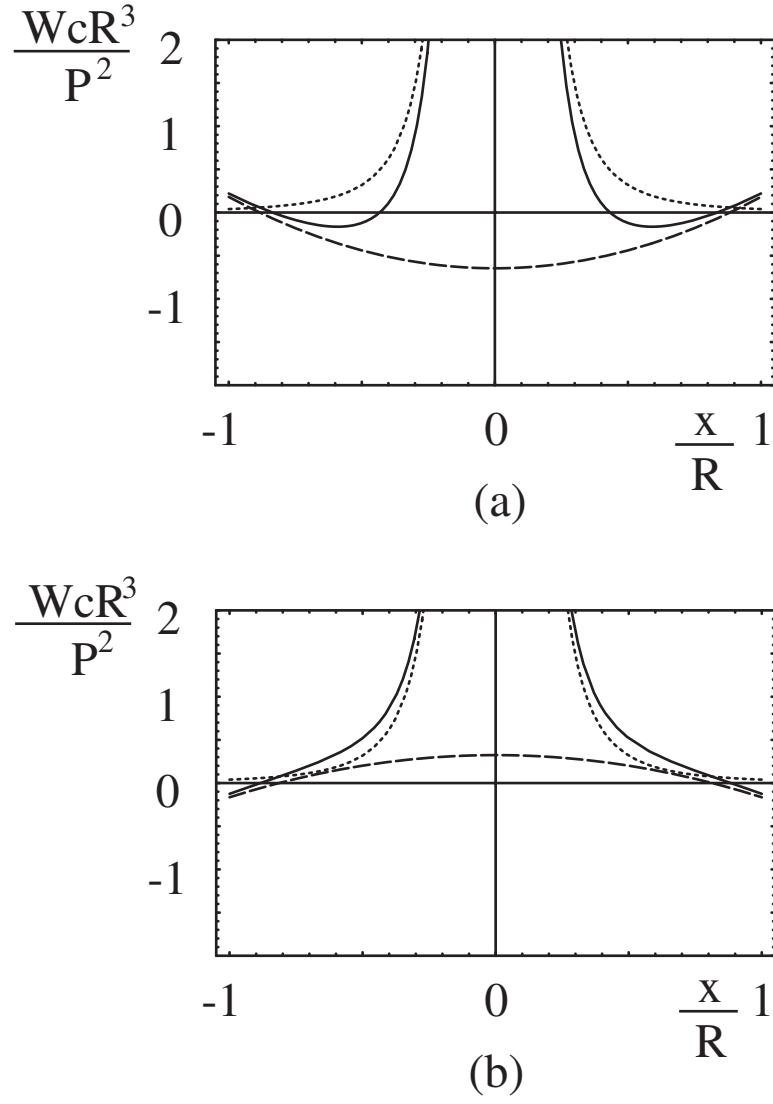


FIG. 2. Elastic interaction energy W in units of P^2/cR^3 for two parallel anisotropic force dipoles of magnitude P in an isotropic elastic sphere with radius R and elastic constants c and $\Lambda = 2$ (Poisson ratio $\nu = 1/3$). For this value of Λ , the direct elastic interaction is repulsive (dotted lines). (a) Free surface: the image correction (dashed line) is attractive and generates a new minimum in the full interaction potential (solid line). (b) Clamped surface: the image correction is repulsive.